Polyurethane-Based Biomaterials for Shape-Adjustable Cardiovascular Devices

A. Silvestri,[1] P. M. Serafini,[1] S. Sartori,[1] P. Ferrando,[1] F. Boccafoschi,[2] S. Milione,[3] L. Conzatti,[4] G. Ciardelli[1]

[1]*Department of Mechanics, Politecnico di Torino, Corso Duca degli Abruzzi 24, 10129 Torino, Italy*
[2]*Department of Clinical and Experimental Medicine, School of Medicine, University of Eastern Piedmont, Via Solaroli 17, 28100 Novara, Italy*
[3]*Department of Chemistry, Università degli Studi di Salerno, Via Ponte Don Melillo, 84084 Fisciano, Italy*
[4]*Istituto per lo Studio delle Macromolecole-Centro Nazionale di Ricerca ISMAC–CNR, Via De Marini 6, 16149 Genova, Italy*

Received 28 April 2011; accepted 28 April 2011
DOI 10.1002/app.34779
Published online 18 August 2011 in Wiley Online Library (wileyonlinelibrary.com).

ABSTRACT: A series of biostable polyurethane (PUR) formulations, including a composite containing a clay as filler, were prepared as new biomaterials for cardiovascular applications. Poly(dimethyl siloxane) and poly(tetramethylene oxide) were selected as macrodiols because of their mechanical properties and the high hydrolysis resistance they confer to PURs. 1,6-Diisocyanatohexane and 1,4-cyclohexane dimethanol were used as a diisocyanate and chain extender, respectively. The polymeric products were chemically, thermally, and mechanically characterized. Thermomechanical characterizations highlighted that some of the obtained formulations are promising materials for applications in the cardiovascular field, in particular, for the realization of annuloplastic rings in mitral valve repair. © 2011 Wiley Periodicals, Inc. J Appl Polym Sci 122: 3661–3671, 2011

Key words: biomaterials; mechanical properties; polyurethanes

INTRODUCTION

Polyurethanes (PURs) belong to the class of thermoplastic elastomers and constitute a very large family of polymers. They can be defined as segmented block copolymers and offer high versatility in terms of formulation design. They generally show a particular morphology, characterized by the presence of two microseparated phases, called the soft and hard phases. The former comprises low glassy transition or low melting soft segments, whereas the latter is made of segments showing a glass-transition temperature (T_g) or crystalline melting temperature (T_m) well above room temperature. This morphology is strictly connected with their excellent mechanical properties, including their high tensile strength and good tear and abrasion resistance. Therefore, PURs have found application in the realization of cardiovascular implantable devices, such as cardiac pacemakers, catheters, prostheses, cardiac assist devices, heart valves, and vascular grafts.[1–3]

For biomedical applications, where material stability is required, poly(dimethyl siloxane) (PDMS)-based PURs present interesting properties. Silicones are a class of polymers that show a low surface energy, hemocompatibility, low toxicity, excellent thermal, oxidative, and hydrolytic stability, and high flexibility. Accordingly, the use of PDMS-based PURs has been proposed in several areas of medical devices, in particular, in the field of cardiovascular prostheses, where blood compatibility and elasticity are the primary requirements. However, if only siloxane is incorporated, the resulting PURs are characterized by very poor mechanical properties.[2,3]

In silicone-containing PURs, it has been observed that remarkable phase separation is not effective in improving mechanical properties: it was reported that the tensile strength and toughness of PDMS-based PURs were lower than those of polyester-based PURs.[4] This behavior can be attributed to the inability of the soft segments to crystallize under strain and to the poor interfacial adhesion between the polar hard regions and the nonpolar soft phases.[5]

Materials with advanced properties can be achieved by the incorporation of both polyether and PDMS as macrodiols in PUR synthesis. The poly(ether)urethane–PDMS elastomeric materials combine the good biocompatibility and mechanical resistance of poly(ether)urethane with the good blood compatibility and long-term biostability of PDMS.

Correspondence to: P. M. Serafini (piero.serafini@polito.it).
Contract grant sponsor: Regione Piemonte, through Bando Regionale-2006 per la Ricerca e lo Sviluppo Precompetitivo; contract grant number: 10-BIADS.

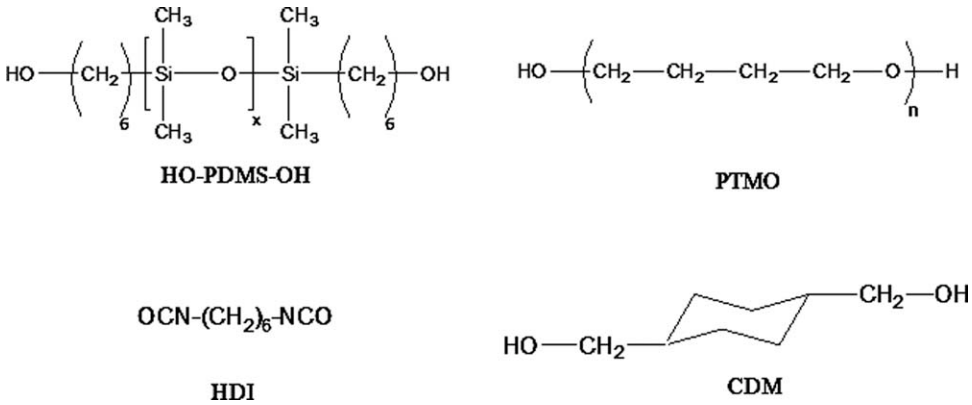

Figure 1 Chemical structures of the reagents used for synthesis of the PDMS/PTMO-based PURs.

The compatibilizing effect between the siloxane-rich soft-segment domains and the urethane-rich hard domains of PURs is attributed to the polyether.[3] Polyether-based PURs have long been considered ideal for many implantable devices, such as blood pump diaphragms, pacemaker lead insulation, and shunts. They are known to have a high biocompatibility and mechanical properties ranging from soft and flexible to hard and rigid. Poly(tetramethylene oxide) (PTMO) is the most common polyether in conventional medical formulations, although it is susceptible to biological oxidation and environmental stress cracking.[6] For this reason, the mechanical properties of PTMO-based PURs can be affected by this degradation process. Nevertheless, it was reported that replacing part of the polyether with polysiloxane seemed to reduce its susceptibility to metal ions[7] and stress cracking.[8]

Further improvements in the mechanical properties were also obtained by the incorporation of a clay filler into the polymeric matrix.[9,10]

In this work, a series of PDMS–PTMO-based PUR formulations are proposed, including a composite containing a clay as a filler, as new biomaterials for cardiovascular applications. In particular, the preparation of a clay composite having a PDMS–PTMO-based PUR as a matrix has never been explored before.

The synthesized PURs were characterized by different molar ratios of PDMS to PTMO in the soft segment. The variation of the chemical composition and the insertion of a clay filler were both aimed at modulating mechanical properties of the polymers to find the proper formulation suitable for biostable cardiovascular devices.

Because it is known that PURs meet the mechanical demands of force-generating contractile tissue, such as the mitralic valve, this work was focused on the development of PUR-based biomaterials to be used in devices showing both elastic and plastic behaviors. A challenging example is given by annuloplastic rings, which have to be capable of accommodating an anatomical saddle shape (plastic response) during surgical implant and mimicking the physiological three-dimensional motion (elastic response) of the native mitral annulus during use.[11]

The PURs were synthesized starting from an aliphatic diisocyanate, namely, 1,6-diisocyanatohexane (HDI), because of its low cost and negligible toxicity of the biodegradation products of its urethane derivates.[12] With regard to the clays used for the preparation of the composites, they were commercial, organomodified montmorillonites. Their organic modifiers are characterized by the presence of long hydrophobic chain(s), often highly effective against a broad spectrum of microorganisms, and widely used as antimicrobial agents.[13] Several studies conducted on these kind of clays have shown their antimicrobial activity, a feature that can turn out to be very useful for implantable devices.

EXPERIMENTAL

PUR synthesis and composite preparation

The PURs were synthesized with a two-step procedure.[14] Two kinds of macrodiols were used: PDMS diol or PDMS [Tegomer H-Si-2311, Evonik (Essen, Germany), number-average molecular weight (M_n) = 2500 g/mol] and poly(tetramethylene oxide) (PTMO; Terethane, Aldrich (St. Louis, MO), M_n = 2000 g/mol; Fig. 1) in different molar ratios: 100 : 0, 80 : 20, 60 : 40, 40 : 60, and 20 : 80. They were dissolved in tetrahydrofuran (THF; Aldrich), and the solution was azeotropically dried. HDI was allowed to react (at a 2 : 1 molar ratio) with the soft segment at 70°C in anhydrous THF to form the prepolymer. At the end of the prepolymer reaction (150 min, with dibutyl tin dilaurate as a catalyst, 1 mol % with respect to the soft segment), the chain extender [1,4-cyclohexane dimethanol (CDM), Aldrich, cis and trans mixture], azeotropically dried in THF, was added at a 1 : 1 molar ratio with respect to

the prepolymer. The chain extension reaction proceeded for 18 h at 25°C. At the end of the polymerization, a given amount of methanol was added to convert the isocyanate end groups to urethane groups. The polymer was collected by double precipitation in distilled water. The second precipitation was performed to remove low-molecular-weight impurities (monomers and oligomers), as confirmed by size exclusion chromatography. After the precipitation, the polymer was washed, filtered, and dried at 40°C under reduced pressure.

The composites were prepared with the solution–intercalation film-casting technique.[15] The clay (Cloisite 30B or Cloisite 20A, Southern Clay Products (Gonzales, TX), 3 and 1 wt %), previously dried in an oven at 100°C for 24 h, was mixed in THF for 8 h. Then, PUR containing 60% PTMO (PU_PTMO60), previously dried in an oven at 40°C for 16 h, was added to the clay solution. It was mixed for 8 h and then cast in a glass Petri dish. The solution was allowed to dry for 1 day. Once dry, the polymer/clay film was placed in a vacuum oven at 40°C for 24 h.

The code used for all of the PURs synthesized is PU_PTMO*X*, where *X* indicates the molar percentage of PTMO in the soft segment; the PDMS content (100% − *X*) is omitted. The code name used for the composites is PU_PTMO*X*–*N*% *Y*, where PU_PTMO*X* is the name of the particular PUR used as the matrix and *N*% and *Y* are the percentage and type, respectively, of clay used.

PUR and composite characterization

M_n and molecular weight distributions (M_w/M_n, where M_w is the weight-average molecular weight) of the PURs were measured by size exclusion chromatography with a Waters 1525 binary system equipped with a Waters 2414 refractive-index detector (Milford, MA). The measurements were performed with four Styragel columns (range = 103–106 Å) at ambient temperature with THF as an eluent (1.0 mL/min); narrow polystyrene standards were used for calibration.

The PUR films were prepared by solvent casting and characterized by attenuated total reflection (ATR)–infrared (IR) spectroscopy and differential scanning calorimetry (DSC). The ATR characterization was performed with a PerkinElmer Spectrum GX Fourier transform infrared system equipped with an ATR attachment (San Jose, CA). The DSC analysis was carried out with a TA Instruments DSC Q20 (New Castle, DE). The DSC curves were obtained by the heating of a sample of about 7 mg from −40 to 280°C at 10°C/min under a nitrogen flow. ^{1}H-NMR spectra were recorded on a Bruke Bruker AVANCE 400 (Billerica, MA) instrument operating at 400 MHz for ^{1}H. The ^{1}H chemical shifts were referenced to $SiMe_4$ with the residual protio impurities of the deuterated solvents as an external reference.

Surface contact angle analysis was made with a KSV CAM2000 (Linthicum Heights, MD) instrument and water as a test liquid. Films of the precipitated PURs were prepared by a hot-press apparatus for subsequent mechanical tests, namely, stress–strain tests and dynamic mechanical thermal analysis (DMTA). Tensile tests at 30–37°C were performed with a TA Instruments DMA Q800. Stress–strain measurements at room temperature were performed with an MTS QTest/10 elite controller (Eden Prairie, MN). The displacement rate was 10 mm/min, and the load limit of the sensor was 500 N. The DMTA tests were performed by a TA Instruments DMA Q800 in the temperature range −80 to +50°C at 1 Hz and at a heating rate of 3°C/min. We performed the creep tests by holding a specimen (film) at a constant uniaxial tensile stress (0.2 MPa) and measuring the resulting compliance (the reciprocal of Young's modulus) and the strain as a function of time (roughly 2000 s) at fixed temperature (37°C). Stress for the creep tests was automatically controlled with the TA Instruments DMA Q800. Composites were characterized by transmission electron microscopy (TEM) and X-ray diffraction (XRD). TEM analysis was performed with a Zeiss EM 900 microscope (Oberkochen, Germany) with the application of an accelerating voltage of 80 kV. Ultrathin sections (ca. 50 nm thick) were obtained with a Leica EM FCS cryoultramicrotome equipped with a diamond knife (sample temperature = −145°C, knife temperature = −60°C). XRD was performed with an Philips X'Pert-MPD XRD diffractometer (Almelo, Netherlands) (Cu Kα radiation, 2θ range = 2–30°; $\Delta 2\theta$ step = 0.02°, step time = 2 s).

Cytotoxicity test: Agar diffusion test

In vitro cytotoxicity analysis was carried out on the PU_PTMO60 sample. The NIH3T3 mouse fibroblast cell line was used. Cells were cultivated in dishes and grown for 24 h at 37°C and 5%CO_2. After a subconfluent cell layer formed, the cells were stained with a vital dye (Neutral Red, Sigma-Aldrich Pty, Castle Hill, Australia) and incubated for 1 h at 37°C and 5% CO_2. Afterward, the staining medium was removed and replaced by Dulbecco's modified eagle medium (DMEM) containing 1.5% agarose. Upon solidification of the agarose, the materials (1 × 1 cm^2) were placed on the top surface of the agar and incubated for 24 h at 37°C and 5% CO_2. Live cells took up the vital staining and retained it, whereas dead cells progressively lost the staining when the viability decreased. The toxicity of the material was evaluated by loss of vital stain under and around the material, and the viability was quantified by extraction of the

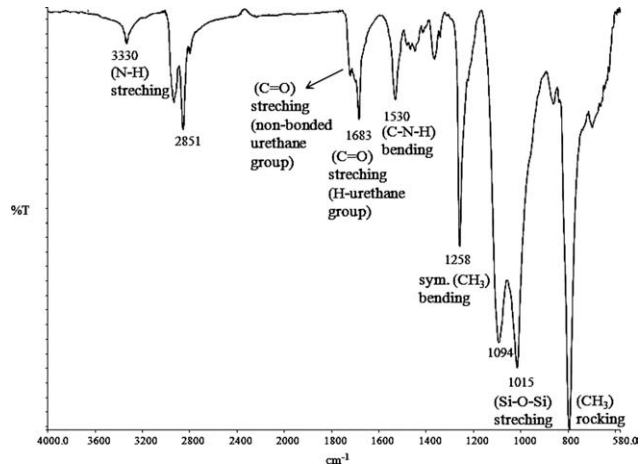

Figure 2 ATR–IR spectrum of PU_PTMO40.

dye with an ethanol (50%)/acetic acid (1%) solution, and the absorbance at 540 nm was read.

RESULTS

PUR synthesis and composite preparation

PDMS–PTMO-based PURs were successfully synthesized, as demonstrated by spectroscopic analysis. In Figure 2, the ATR–IR spectrum of PU_PTMO40 is reported. It shows the characteristic peaks of the PURs containing PDMS and PTMO in the soft segment:[5] 1683 cm^{-1} (urethane C═O), 3330 cm^{-1} (urethane N—H, hydrogen bonded), 1530 cm^{-1} (urethane N—H, not hydrogen bonded). The presence of PDMS was shown by the double peak of Si—O—Si stretching at 1100 cm^{-1}. The C—O—C stretching band was not visible because it was probably covered by the large and strong Si—O—Si stretching band. Both vibrations occur at the same wave-number value. ^{1}H-NMR was used to confirm the PTMO presence in the polymer chain. In Figure 3, the ^{1}H-NMR spectrum of PU_PTMO40 is shown. The signal at 3.4 ppm corresponded to the —O—CH_2— group of the polyether and was not present in the ^{1}H-NMR spectrum of PUR containing PDMS only.

TABLE I
Experimental Data from the PUR Syntheses

Sample	$M_n \times 10^3$ (g/mol)	M_w/M_n	Yield (%)
PU_PTMO20	20	1.4	81
PU_PTMO40	26	2.0	80
PU_PTMO60	24	1.5	85
PU_PTMO80	26	1.6	90

The experimental data concerning the molar composition, molecular weights, polydispersity index (M_w/M_n), and reaction yields of the obtained PDMS–PTMO-based PURs are collected in Table I.

The composites were obtained as shown by TEM and XRD analysis. In Figure 4, TEM images of PU_PTMO60–3% 30B are reported as an example. The hard phase (gray) of the PUR matrix was highlighted by RuO_4 vapor, and the clay seemed to interact preferably with the soft phase (white), showing a low grade of intercalation. The preferential interaction of the clay with the more apolar phase could be explained by consideration of the organic nature of

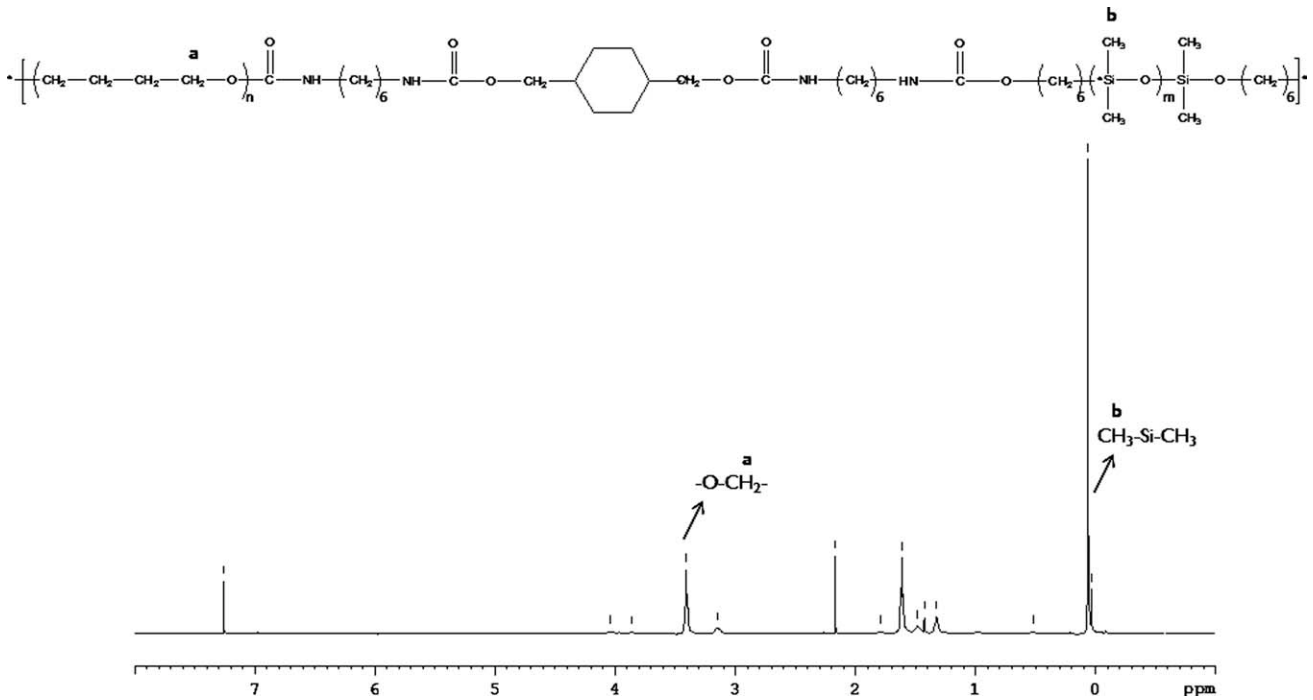

Figure 3 ^{1}H-NMR spectrum of PU_PTMO40.

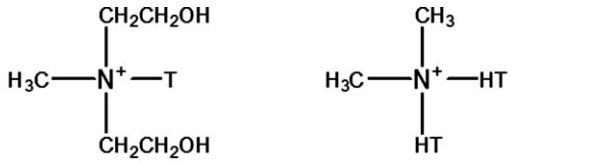

Bis(2-hydroxy-ethyl)methyl tallow ammonium

Dimethyl bis(hydrogenated-tallow) ammonium

Figure 4 Chemical structures of the organic cations of the clays Cloisite 30B [bis(2-hydroxyethyl)methyl tallow ammonium] and Cloisite 20A [dimethyl bis(hydrogenated tallow)ammonium]. The tallow composition was as follows: ~ 65% C18, ~ 30% C16, and ~ 5% C14.

the clay surface: Cloisite30B is a organophilic montmorillonite modified through the ionic exchange of the sodium interlayer cation with an organic cation, namely, a bulky alkylammonium [bis(2-hydroxyethyl)methyl tallow ammonium, where the tallow composition was as follows: ~ 65% C18, ~ 30% C16, and ~ 5% C14, which acted as a surface modifier. By increasing the interlayer spacing and making the clay more compatible with organic polymers, these alkylammonium ions allowed the polymer chains to diffuse between the layers. The nature of the organic cation had a significant effect on the resulting morphology of the nanocomposite (Fig. 5).[15]

Because of the low grade of intercalation, the obtained product could be defined as a microcomposite because the major part of the clay was present in the form of microaggregates (<3 μm). This result was confirmed by XRD. In the XRD spectrum reported as an example [Fig. 6(b)], one peak for Cloisite 30B at $2\theta = 5^\circ$, in the same position as for the single clay, and two broadened peaks relative to the PUR matrix at $2\theta = 12$ and 20° were observed.[16] The absence of a shift for the Cloisite peak indicated that the clay layers were not affected by polymer intercalation, whereas the two broadened peaks were probably due to an increased disorder of the polymeric chains with respect to the pure PUR [Fig. 6(a)].

Surface properties: Contact angle analysis

Contact angle measurements demonstrated the high hydrophobicity of the synthesized PURs and the prepared composites. In particular, the contact angle values of the PURs, collected in Table II, decreased with the reduction of siloxane content in the sample.

In the same table, the contact angle values of the composites are reported. It could be observed that the insertion of a clay filler slightly increased the hydrophobicity of the samples: for example, the composite PU_PTMO60–3% 30B showed a contact angle value higher than its correspondent pure matrix (PU_PTMO60), which could have been an effect of the nonpolar tails of the organic ammonium salt modifier. The sample PU_PTMO60–1% 20A exhibited the highest contact angle value among all of the composites because of the higher hydrophobicity of Cloisite 20A with respect to Cloisite 30B (see Fig. 5).[17]

Thermal and mechanical characterization

DSC and DMTA

From DSC and DMTA, it was observed that the obtained PURs were characterized by a three-phase

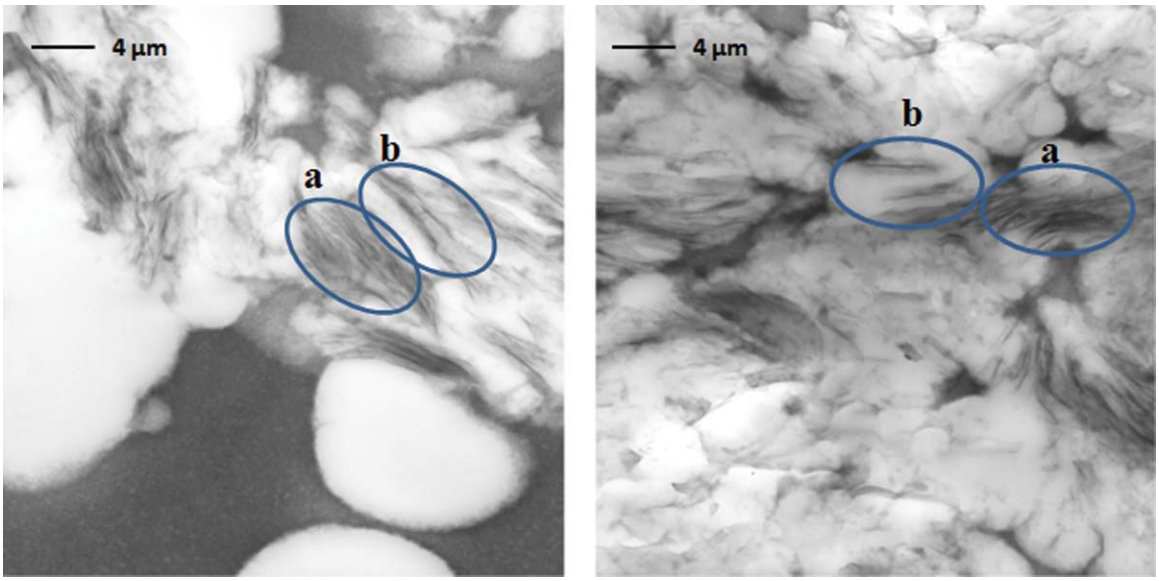

Figure 5 TEM images of the composite PU_PTMO60–3% 30B. The soft phase (white) and hard phase (gray) were evidenced by RuO_4 vapor. (a) Parts in which a microclay arrangement was observable. (b) Parts in which an intercalation process was evident. [Color figure can be viewed in the online issue, which is available at wileyonlinelibrary. com.]

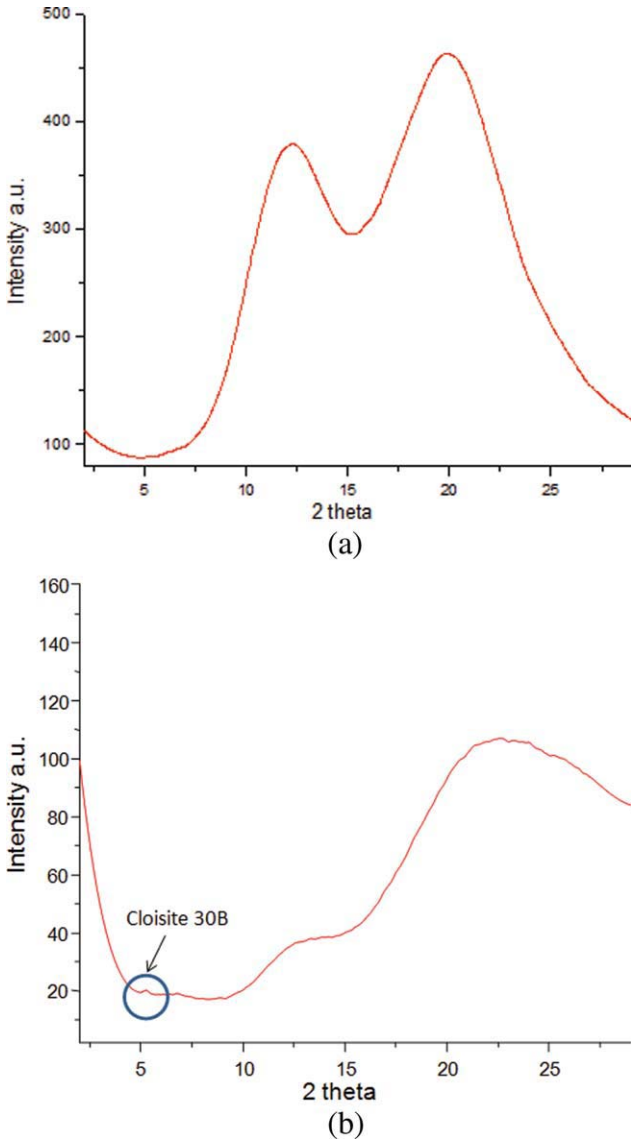

Figure 6 XRD spectra of (a) PU_PTMO60 and (b) PU_PTMO60–3% 30B. [Color figure can be viewed in the online issue, which is available at wileyonlinelibrary.com.]

morphology, typical of PDMS–PTMO-based PURs. Generally, it is possible to detect the siloxane phase, the hard phase, and a polyether-rich phase, which can include some hard segments.[18,19] This separation was more evident in the polymers containing the higher percentage of siloxane and tended to disappear with increasing polyether content. In Figure 7, the thermal

TABLE II
Contact Angle Values of the PUR Formulations

Sample	Contact angle (°)
PU_PTMO40	112.9 ± 0.4
PU_PTMO60	102.9 ± 0.4
PU_PTMO80	101.2 ± 0.4
PU_PTMO60–3% 30B	105.4 ± 0.4
PU_PTMO60–1% 30B	103.5 ± 0.4
PU_PTMO60–1% 20A	107.8 ± 0.4

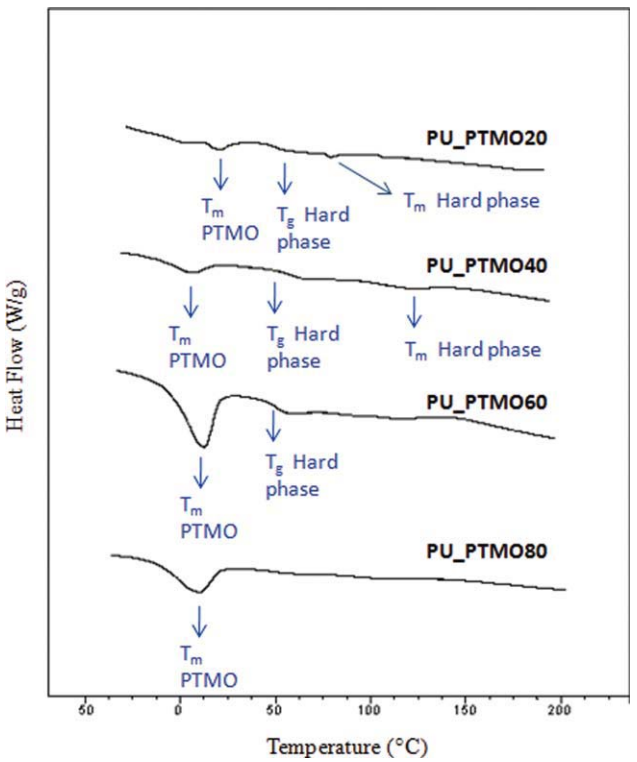

Figure 7 DSC thermograms of the synthesized PURs. [Color figure can be viewed in the online issue, which is available at wileyonlinelibrary.com.]

curves of the synthesized PURs are reported. In these curves, the glass transitions of the PDMS phases were not visible, and the T_g values relative to these phases were obtained by DMTA and are collected in Table III. By observing the thermal curve relative to PU_PTMO20, we could detect T_m of the PTMO phase at 19°C and T_g and T_m of the hard phase at 46 and 77°C, respectively. The PU_PTMO40 curve showed a similar trend to PU_PTMO20, but it was characterized by a less marked melting peak for the hard phase. The PU_PTMO60 curve showed a PTMO melting peak (14°C) and T_g of the hard phase (49°C). In the DSC curve of PU_PTMO80, only T_m of PTMO was detectable, whereas T_g and T_m of the hard phase were not visible. Therefore, with decreasing PDMS content, the transition ascribable to the hard phase became less evident and disappeared in the polymer with the

TABLE III
Experimental Data from DSC and DMTA

	T_m (°C)		T_g (°C)	
Sample	PTMO (DSC)	Hard phase (DSC)	Hard phase (DSC)	Soft phase (DMTA)
PU_PTMO20	19	77	46	−80
PU_PTMO40	20	119	60	−67
PU_PTMO60	14	—	49	−65
PU_PTMO80	8.7	—	—	−63

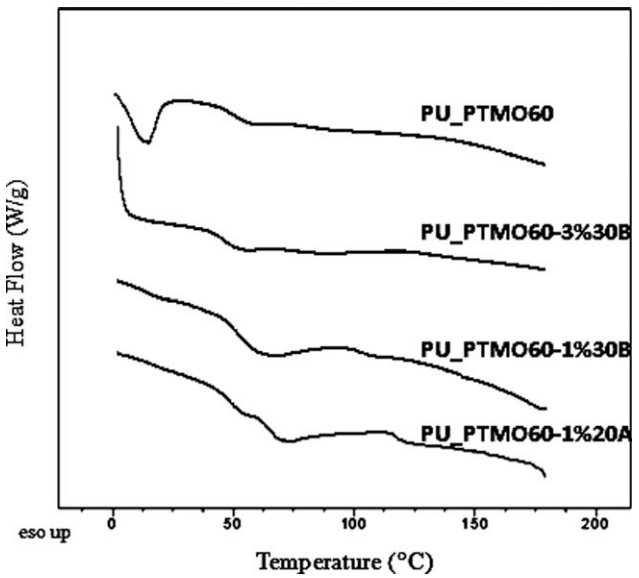

Figure 8 DSC thermograms of PU_PTMO60 and its composites.

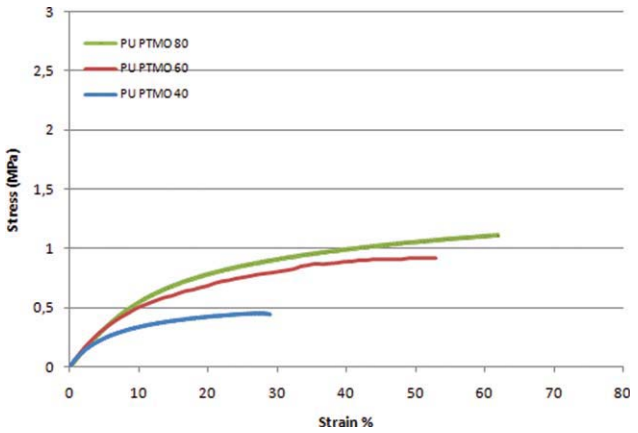

Figure 9 Stress–strain curves of the synthesized PURs with different percentages of PTMO in the soft segment. [Color figure can be viewed in the online issue, which is available at wileyonlinelibrary.com.]

highest PTMO content. The reduction of phase separation was also indicated by increasing PDMS phase T_g values (Table III). T_g was influenced by the purity of the phase; therefore, in the case of marked phase separation, T_g was found at a value that was very close to T_g of the respective soft-segment macrodiol.[20] With decreasing siloxane content in the PUR chains, the corresponding T_g became increasingly different from the T_g of the pure PDMS diol (−110°C, −80°C for PU_PTMO20, −63°C for PU_PTMO80).

DSC thermograms of the composites are reported in Figure 8 and compared with the thermal curve of the pure matrix, PU_PTMO60. As previously mentioned, this polymer exhibited the melting peak of PTMO at 14°C that was completely absent in the curves of all of the composites. The absence of this signal was probably due to the presence of the clay, which hindered the crystallization of the PTMO segments.

Stress–strain tests

The PURs were characterized by stress–strain tests, and the results are reported in Table IV and Figure 9, with the exception of PU_PTMO20, which was not processable for obtaining measurable specimens. From the stress–strain curves, it was observed that a higher percentage of PTMO in the soft segment improved the mechanical performances of PURs, increasing Young's modulus, the stress at break, and the maximum strain.

In Table IV, it is possible to observe that the insertion of the clay into the PUR matrix (PU_PTMO60) led to an improvement in the mechanical properties only in the case of 1% Cloisite 30B. These data could be explained by consideration of the nature of the clay and its relative amount. Cloisite 30B is characterized by a more polar ammonium cation than Cloisite 20A (see Fig. 5), which was expected to interact better with the PUR PTMO-rich soft phase.[12] With regard to the clay content, it was possible to assume that a lower amount of the filler allowed it to have better dispersion and intercalation.[21]

In particular, Young's modulus increased approximately 10 and 55% of the initial value when the ratio of PTMO to PDMS shifted from 40/60 to 60/40 and from 60/40 to 20/80 in the soft segment, respectively, as shown in Figure 10. Similarly, for the stress at break, there were improvements of 80 and 33%, respectively, of the initial value, which resulted from the increase in the PTMO percentage from 40 to 60% and 60 to 80%, respectively. The maximum strain percentage increase

TABLE IV
Mechanical Properties of the Synthesized PURs and Composites

Sample	Young's modulus at 30°C (MPa)	Strain at break (%)	Stress at break (MPa)
PU_PTMO20	—	—	—
PU_PTMO40	5.0 ± 0.1	30 ± 3.4	0.5 ± 0.1
PU_PTMO60	5.5 ± 0.4	55 ± 5	0.9 ± 0.2
PU_PTMO80	9.0 ± 0.7	62 ± 8	1.2 ± 0.2
PU_PTMO60–1% 30B	8.3 ± 0.3	30 ± 2	1.0 ± 0.1
PU_PTMO60–3% 30B	5.1 ± 0.3	52 ± 1.4	1.0 ± 0.3
PU_PTMO60–1% 20A	5.2 ± 0.4	55 ± 5.5	1.2 ± 0.4

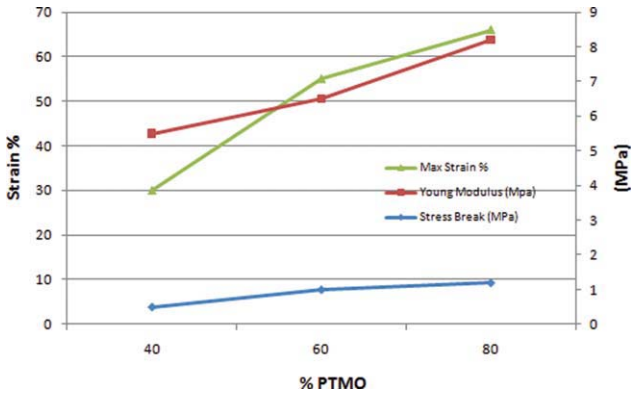

Figure 10 Influence of the PTMO content on the Young's modulus, strain percentage, and stress at break. [Color figure can be viewed in the online issue, which is available at wileyonlinelibrary.com.]

(ca. 80% of the initial value) was observed when the amount of PTMO increased from 40 to 60%.

Time and temperature dependence of the mechanical properties

Creep and stress–strain tests at 37°C were performed to evaluate the viscoelastic properties of the PURs and their composites at human body temperature. During the creep test, the compliance (the reciprocal of Young's modulus) and the strain percentage as a function of time at 37°C (physiological temperature) were measured. The synthesized PDMS–PTMO PURs and the composites were also found to exhibit evident viscoelastic behavior. The compliance of the synthesized PDMS–PTMO-based PURs and the composites realized with PU_PTMO60 are shown in Figures 11 and 12, respectively.

The curves of Figure 11 show a very different trend for PU_PTMO40, PU_PTMO60, and PU_PTMO80. The compliance for the PUR with the lowest amount of PTMO seemed to increase more

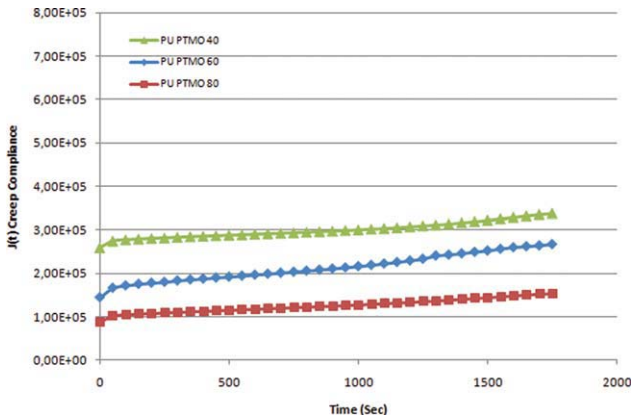

Figure 11 Creep compliance as a function of time at 37°C. [Color figure can be viewed in the online issue, which is available at wileyonlinelibrary.com.]

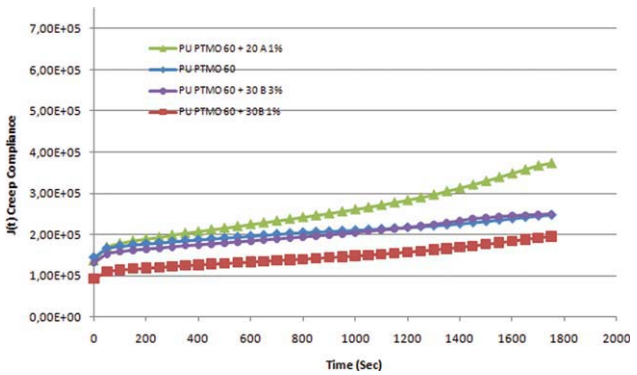

Figure 12 Creep compliance as a function of time at 37°C. [Color figure can be viewed in the online issue, which is available at wileyonlinelibrary.com.]

quickly than for those for PU_PTMO60 and PU_PTMO80. Therefore, the better viscoelastic behavior and the less pronounced decrease in Young's modulus as a function of time seemed to be related to the highest percentage of PTMO. The same trend can also be observed in Figure 12, which shows the compliance as a function of time for PU_PTMO60 and the composites realized with Cloisite 30B and 20A. There was an important improvement in the compliance for PU_PTMO60 and for the composite based on 3% Cloisite 30B with respect to the same composite with 1% filler, as shown by the slopes of the curves. This trend was also confirmed by the results reported in Table V. Otherwise, the compliance of the composite based on Cloisite 20A showed a more pronounced improvement at the highest creep times, as compared with PU_PTMO60. Furthermore, the creep strain was analyzed for each sample. The absolute creep strain ($\Delta\varepsilon$) was equal to the sum of the delayed elastic deformation (ε_2) and the permanent elastic deformation (ε_3; Fig. 13). In Figure 14, the $\Delta\varepsilon$ percentage for each sample is shown. These values seemed to confirm the trend observed, in particular, that with the increase in the PTMO content, the $\Delta\varepsilon$ decreased. Moreover, the

TABLE V
Mechanical Properties of the Synthesized PURs

Sample	Young's modulus at 30°C (MPa)	Young's modulus at 37°C (MPa)	Decrease in Young's modulus with temperature (%)
PU_PTMO20	—	—	—
PU_PTMO40	5.0 ± 0.1	4 ± 0.3	25
PU_PTMO60	5.5 ± 0.4	4.3 ± 0.4	27
PU_PTMO80	9.0 ± 0.7	7.8 ± 0.6	15
PU_PTMO60–1% 30B	8.3 ± 0.3	7.3 ± 0.3	13
PU_PTMO60–3% 30B	5.1 ± 0.3	4.1 ± 0.1	25
PU_PTMO60–1% 20A	5.2 ± 0.4	4.7 ± 0.5	10

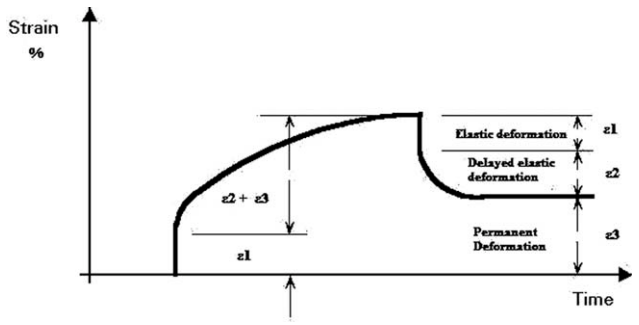

Figure 13 Schematic representation of a creep curve as a function of time (ε_1 = elastic deformation).

PUR containing 1% Cloisite 30B showed the lowest creep value according to the results of the compliance.

The behavior of the prepared PURs was found to be temperature- and humidity-dependent, as was reported in the literature.[22] In this study, the influence of the temperature on Young's modulus was evaluated. In fact, the modulus was measured at 37 and at 30°C for samples with different PTMO and filler contents (Table V).

Cytotoxicity test: Agar diffusion test

The use of an indirect cell contact test was chosen to evaluate the eventual environmental toxicity due to the presence of the material. An agar diffusion test, performed with the NIH3T3 mouse fibroblast cell line, showed that cell viability on the PU_PTMO60 after 24 h was about 61% respect to the control (see Fig. 15). This indicated that after 24 h, the cells maintained a good viability with a weak decrease with respect to the control cells. PU_PTMO60 was chosen as test material because the mechanical analysis showed that this polymer had suitable properties for the realization of the annuloplastic device.

DISCUSSION

The synthesized PURs showed Young's modulus values at 30°C to range between 5 MPa and roughly 9 MPa. An increase in the temperature from 30 to 37°C (human body temperature) resulted in about a 23% decrease in Young's modulus (on average), as shown in Table V. The creep test results showed an important stability of Young's modulus at 37°C, especially for PU_PTMO80. The insertion of the clay filler improved the mechanical properties because the elastic modulus and the stress at break increased, especially for the sample containing 3% Cloisite 30B. Also, in this case, a decrease in Young's modulus at 37°C (16% on average, lower than that of the PURs) was observed.

The composites showed a different viscoelastic behavior, depending on the nature of the inorganic filler. In particular, composites containing Cloisite 30B (1–3%) seemed to be more stable in terms of Young's modulus with respect to the same PUR having Cloisite 20A as a filler.

The fine tuning of the mechanical properties is a key issue in the design of materials for implantable biomedical devices. The material has to comply with the procedure used by the surgeon during implant and with the mechanical solicitation of the surrounding tissues. As already stated in the Introduction, cardiovascular applications have very strict requirements that are difficult to fulfill.[23]

The mechanical behavior of the prepared formulations demonstrated that these biomaterials seem to be suitable for annuloplastic applications. In fact, the Young's modulus values of natural mitral valve tissue are roughly 6 MPa in the circumferential (parallel to the annulus) direction and 2 MPa in the longitudinal (perpendicular to the annulus) direction.[22] Stress values measured in the elastic region were in the range of those expected during heartbeat evaluation in an *in vivo* study.[25,26]

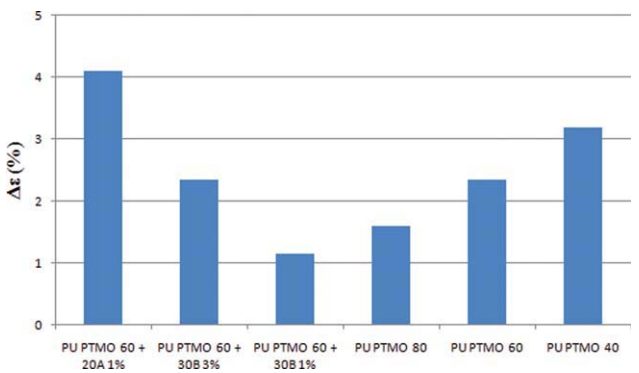

Figure 14 Δε percentage at 37°C. [Color figure can be viewed in the online issue, which is available at wileyonlinelibrary.com.]

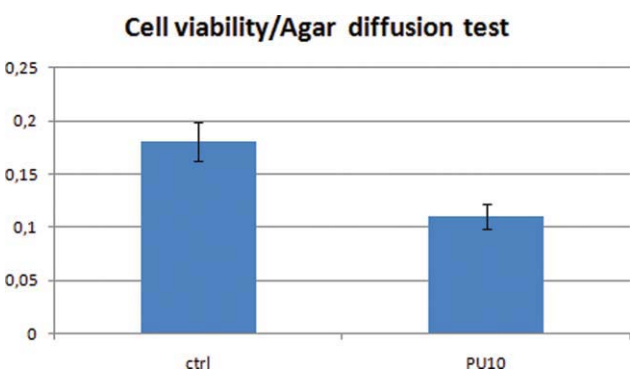

Figure 15 Agar diffusion test. [Color figure can be viewed in the online issue, which is available at wileyonlinelibrary.com.]

The creep behavior showed a quite stable trend of the elastic modulus and the absolute strain percentage at 37°C for several formulations.

Therefore, it is expected that the formulation prepared will be suitable to realize devices whose shape can be adapted to the anatomical shape when implanted and will then show an elastic behavior during use and maintain their dimensional stability with time.

The mitral annulus is characterized by several regions that are subject to different mechanical forces. Therefore, it is important to modulate the mechanical response of the material used for this kind of device.[27] A thermoplastic polymeric material con be molded into shapes with regions of different sections, to comply with the different solicitation that they will undergo *in vivo*. So far, the best results in this context have been obtained by the use of metallic materials.[23] The polymeric biomaterials proposed in this work provide an alternative approach that is perceptively cheaper and more viable with respect to existing technologies.

Moreover, these materials turn out to be innovative respect with available commercial PUR formulations because of the use of nonaromatic diisocyanate[28] in the synthesis process. These aliphatic components will allow us to obtain mechanical properties very close to those of the native mitralic tissue and, in the unlikely case in which the polymer is affected by the degradation processes, will avoid the production of highly toxic aromatic diamines.[29]

The prepared materials were designed to form the soft inner core of the device (mitral ring) and to be covered with a medical-grade polymer fabric [e.g., poly(ethylene terephthalate)] to ensure the suturability and with a carbofilm layer to ensure hemocompatibility and antithrombogenicity and to minimize inflammatory response.[30] As they are not expected to be in direct contact with cells, we chose to perform a toxicity analysis by an agar diffusion test. This kind of test showed good results in terms of fibroblast viability for PU_PTMO60, which was selected for its suitable mechanical behavior.

CONCLUSIONS

In this study, a series of PDMS–PTMO-based PURs and clay composites were successfully achieved, as demonstrated by spectroscopic analysis. Thermomechanical characterizations of the obtained formulations highlighted that the proposed formulations seem to be suitable for mitralic applications, in particular, for annuloplastic rings. The Young's modulus values at 37°C were all included in the range required for the realization of these kinds of devices. In detail, it could be possible to choose two or more materials characterized by different elastic modulus values to combine them in the realization of the parts of the ring. Alternatively, the same material could be molded in regions of different sections to modulate the mechanical properties.

With the creep tests taken into consideration, the best PUR-based formulations turned out to be the PURs containing 60 and 80% PTMO in the soft segment (PU_PTMO60 and PU_PTMO80) and the composites containing Cloisite 30B as a filler (1 and 3%).

Further works are in progress to test these materials in cycling fatigue conditions and to demonstrate their processability from the melt to produce prototypes of PUR-based annuloplastic rings. Moreover, the influence of the humidity on the mechanical properties for these PURs will be evaluated and clarified in a future work, together with a modeling study for fitting the creep data with a viscoelastic model.

Additional investigation into the composites preparation will be performed to improve the rate of intercalation. The study should provide additional information for the fine tuning of the functional properties in the formulation.

The authors thank G. Colucci of Politecnico di Torino for his technical support in XRD analysis.

References

1. Gunatillake, P. A.; Meijs, G. F.; Mccarrthy, S. J. S.; Adhikari, R. J Appl Polym Sci 2003, 56, 545.
2. Wang, F. Ph.D. Thesis, Virginia Polytechnic Institute, 1998.
3. Gunatillake, P. A.; Gordon, F.; Meijs, G. F.; Simon, J.; Mccarrthy, S. J.; Adhikari, R. J Appl Polym Sci 2000, 76, 2026.
4. Speckhard, T. A.; Cooper, S. L. Rubber Chem Technol 1986, 59, 405.
5. Park, H. B.; Kim, C. K.; Lee, Y. L. J Membr Sci 2002, 204, 257.
6. Stachelek, S. J.; Alferiev, I.; Choi, H.; Chan, C. W.; Zubiate, B.; Sacks, M.; Composto, R.; Chen, I.; Levy, R. J. J Biomed Mater Res A 2007, 82, 1004.
7. Ward, B.; Anderson, J.; Ebert, M.; McVenes, R.; Stokes, K. J Biomed Mater Res A 2006, 77, 380; Xiong, J.; Zheng, Z.; Jiang, H.; Ye, S.; Wang, X. Compos A 2007, 38, 132.
8. Anderson, J. M.; Hiltner, A.; Wiggins, M. J.; Mark, A.; Schubert, M. A.; Collier, T. O.; Kao, J. W.; Mathur, A. B. Polym Int 1998, 46, 163.
9. Zeng, Q. H.; Yu, A. B.; Lu, G. Q. M.; Paul, D. R. J Nanosci Nanotechnol 2005, 5, 1574.
10. Utracki, L. A. Clay-Containing Polymeric Nanocomposites; Rapra Technology: Shropshire, United Kingdom, 2004; Vol. 1.
11. Arita, M.; Kasegawa, H.; Mitsuo Umezu, M. Asian Cardiovasc Thorac Ann 2001, 9, 14.
12. Sartori, S.; Rechichi, A.; Vozzi, G.; D'Acunto, M.; Heine, E.; Giusti, P.; Ciardelli, G. React Funct Polym 2008, 68, 809.
13. Nigmatullin, R.; Gao, F.; Konovalova, V. J Mater Sci 2008, 43, 5728.
14. Ciardelli, G.; Rechichi, A.; Sartori, S.; D'Acunto, M.; Caporale, A.; Peggion, E.; Vozzi, G.; Giusti, P. Polym Adv Technol 2006, 17, 786.
15. Herrera-Alonso, J. M.; Maranda, E.; Little, J. C.; Cox, S. S. J Membr Sci 2009, 337, 208.
16. Bokobza, L. J Appl Polym Sci 2004, 93, 2095.
17. Pegoretti, A.; Dorigato, A.; Brugnara, M.; Penati, A. Eur Polym J 2008, 44, 1662.

18. Lin, Y.-H.; Chou, N.-K.; Chen, K.-F.; Ho, G.-H.; Chang, C.-H.; Wang, S.-S.; Chu, S.H.; Hsieh, K.-H. Polym Int 2007, 56, 1415.
19. Choi, T.; Weksler, J.; Padsalgikar, A.; Runt, J. Polymer 2009, 50, 2320.
20. Lamba, M. K. N.; Woodhouse, K. A.; Cooper, L. S. Polyurethanes in Biomedical Applications; CRC: Boca Raton, FL, 1998; Chapter 4.
21. Xiong, J.; Zheng, Z.; Jiang, H.; Ye, S.; Wang, X. Compos A 2007, 38, 132.
22. Kanyantaa, V.; Ivankovi, A. J Mech Behav Biomed Mater 2010, 3, 51.
23. Ferris, M. Ph.D. Thesis, North Carolina State University, 2009.
24. Votta, E.; Maisano, F.; Montevecchi, F. M. Ann Thorac Surg 2007, 84, 92.
25. Jensen, M.; Jensen, H.; Nielsen, S. L.; Smerup, M. J Heart Valve Dis 2008, 17, 267.
26. Ferrazzi, P.; Iacovoni, A.; Pentiricci, S. J Thoracic Cardiovasc Surgery 2009, 137, 174.
27. Daebritz, S. H.; Fausten, B.; Hermanns, B. Heart Surgery Forum 2004, 7, 5.
28. Martin, D. J. A.; Poole, L. A.; Gunatillake, P. A.; McCarthy, S. J.; Meijs, G. F.; Schindhelm, K. Biomaterials 2000, 21, 1021.
29. Tuominen, J.; Kylmä, J.; Kapanen, A.; Venelampi, O.; Itavaara, M.; Seppala, J. Biomacromolecules 2002, 3, 445.
30. Della Barbera, M.; Laborde, F.; Thiene, G.; Arata, V.; Pettenazzo, E.; Pasquino, E.; Behr, L.; Valente, M. Cardiovasc Pathol 2005, 14, 96.